

Theory of structural, electronic, vibrational, and superconducting properties of high-pressure phases of sulfur

Oleg Zakharov and Marvin L. Cohen

*Department of Physics, University of California at Berkeley and Materials Sciences Division,
Lawrence Berkeley Laboratory, Berkeley, California 94720*

(Received 5 June 1995)

Pseudopotential *ab initio* calculations are performed for three high-pressure phases of sulfur (bco, β -Po, and bcc). These calculations yield a value of around 550 GPa for the transition pressure of the β -Po to bcc transformation; however, we do not reproduce the reported bco to β -Po phase transition. *Ab initio* calculations of the phonon spectrum and the electron-phonon interaction for the bcc phase of sulfur are also done using the frozen phonon method. The results predict that the bcc phase of sulfur is a metal with very low resistivity and a superconducting transition temperature of 15 K.

I. INTRODUCTION

The high-pressure properties of group VIA elements are currently a subject of renewed experimental research,¹⁻⁷ and the purpose of this paper is to provide theoretical studies for comparison and to motivate future work. The high-pressure behavior of some of these elements, such as Se and Te, is relatively well established.^{1,2,4} Under pressure both undergo a number of structural phase transitions and become metallic. The higher-pressure end of the transition sequence is similar for both Se and Te. With increasing pressure, these elements transform from a base-centered orthorhombic phase (bco) to a β -Po primitive rhombohedral structure and then to a close-packed bcc phase. A number of *ab initio* calculations have been performed for Se and Te,⁸⁻¹⁰ which generally give results in reasonably good agreement with the experimental data [with a notable exception of the bulk modulus for the bcc phase of Te (Ref. 10)].

Although sulfur is expected to exhibit a similar sequence of high-pressure phases, because of the much higher pressures required, until recently the experimental determination of these phases was not possible. The metallic bco phase of sulfur was first observed in optical studies³ and later confirmed by x-ray-diffraction experiments.^{6,7} This phase becomes stable at about 90 GPa. The extension of the pressure range to 212 GPa (Ref. 7) allowed the observation of the transition to the β -Po phase at a pressure of 162 GPa. The bcc phase of sulfur has not yet been observed experimentally.

In this paper we present the results of *ab initio* pseudopotential calculations for high-pressure phases of sulfur. Using the total-energy formalism¹¹ we predict that the phase transition from the β -Po to the bcc phase will occur at about 550 GPa. We also find the total energy of the bco phase to be higher than that of the β -Po phase; hence our calculations do not reproduce the reported bco to β -Po transition.

The metallic phases of both Se and Te are known to be superconducting at low temperatures.¹²⁻¹⁴ To explore this possibility for sulfur, we performed "frozen phonon" calculations of the electron-phonon interaction constant for the hypothetical bcc phase of S. These calculations allow us to estimate T_c and the high-temperature value of the resistivity

for this phase. According to our calculations, at high pressure sulfur is a good metallic conductor with very low resistivity, and we estimate T_c for the bcc structure at a pressure of 585 GPa to be 15 K. The enhancement of the electron-phonon interaction near the bcc-to- β -Po structural transition contributes into this value.

This paper is organized as follows. In Sec. II we briefly outline the theoretical method for the total-energy calculations and present our results for the structural and electronic properties of high-pressure phases of sulfur. Sec. III is devoted to a calculation of the phonon dispersion curves and the electron-phonon interaction constants for the bcc phase of sulfur using the frozen phonon method. A summary is given in Sec. IV.

II. STRUCTURAL AND ELECTRONIC PROPERTIES OF SULFUR AT HIGH PRESSURE

A. Method

The structural properties of high-pressure phases of sulfur are calculated using the standard plane-wave pseudopotential approach in the local-density approximation (LDA).¹¹ The sulfur pseudopotential was generated by the Troullier-Martins¹⁵ method with semirelativistic corrections. The Ceperley-Alder¹⁶ form is used for the exchange potential.

Different cutoff energies are used for the different structures. The three lattice parameters of the bco phase are optimized for a fixed volume using the steepest decent minimization algorithm. The derivatives of the total energy with respect to the lattice parameters are found using the calculated Hellmann-Feynman forces and stresses.¹¹ A cutoff energy of 35 Ry and 216 special \mathbf{k} points¹⁷ in the irreducible part of the Brillouin zone generated using the Monkhorst-Pack scheme¹⁸ are used in this calculation. The total energy for the optimized lattice parameters is calculated with a cutoff energy of 60 Ry. For the β -Po structure, the c/a ratio is optimized for a fixed volume. A cutoff energy of 60 Ry with 280 \mathbf{k} points in the irreducible part of the Brillouin zone is used. Calculations for the bcc structure are performed with a 90-Ry cutoff and 250 irreducible \mathbf{k} points. The total energies obtained are fit to the Murnaghan equation of state.¹⁹

B. Results

In this section we consider the structural and electronic properties of sulfur in the orthorhombic (bco), rhombohedral (β -Po), and bcc high-pressure phases. As a model for the crystal structure of the high-pressure S-III phase of sulfur we have chosen the puckered layer structure proposed for the orthorhombic (Se-IV) phase of selenium.⁴ In our calculations we assume that the zigzag bonds forming the the puckered layers are of equal length; hence this structure has two atoms per unit cell. The calculations for a more general structure with the zigzag bonds of unequal length were reported for Te in Ref. 10.

Using energy minimization, we determine the optimized lattice parameters for the bco structure. The calculated parameters are within a few percent of the experimental values. For example, for an atomic volume of 8.817 \AA^3 , the calculated (experimental²⁰) lattice parameters are $a=3.398$ (3.309) \AA , $b=4.878$ (4.970) \AA , $c=2.128$ (2.145) \AA , $u=0.119$ (the quantity $2ub$ gives the width of the puckered layer which was not determined experimentally). The calculated pressure using the equation of state for this volume is 148 GPa; the experimental value is 143 GPa.

The β -Po structure can be described as a simple cubic lattice deformed along the $[111]$ direction keeping the edges unchanged. The angle α between the edges is not equal to 90° after the deformation. For $\alpha=109^\circ 28'$, the β -Po structure coincides with the bcc structure. The β -Po structure can also be considered as a hexagonal lattice with three atoms per unit cell and ABC stacking.

The agreement of the optimized lattice parameters with the experimental value is very good for the β -Po structure. For an atomic volume of 8 \AA^3 , the calculated angle minimizing the total energy of the β -Po structure is $\alpha=103.99^\circ$ [the experimental value is $\alpha=104.03^\circ$ (Ref. 20)] at the calculated pressure of 203 GPa (212 GPa in the experiment).

The total energies versus volume curves for the β -Po and bcc phases of S are given in Fig. 1. According to our calculations, the transition pressure from the β -Po to the bcc phase is 545 GPa. The relative change of the cell volume is less than 1%. This means that the angle α increases with pressure almost up to the bcc value of $109^\circ 28'$, and the transition takes place with small change of the angle. We note here that the nearly second-order character of the β -Po-to-bcc phase transition reduces the accuracy of the calculated transition pressure, since small errors in the calculated total energies may result in significant changes in the transition pressure.

The calculated total energy for the bco phase is higher by approximately 4 mRy/atom than the total energy of the β -Po structure with the same atomic volume in the region where the bco phase is reported experimentally. Two of the calculated total energies for the bco phase of S are presented in the inset in Fig. 1. The first point corresponds to a pressure of about 75 GPa and the second corresponds to a pressure of 145 GPa. The position of these two points suggests that the calculated total-energy curve for the bco structure is higher in energy than the β -Po for the whole range of pressure where the bco phase is observed in the experiment.

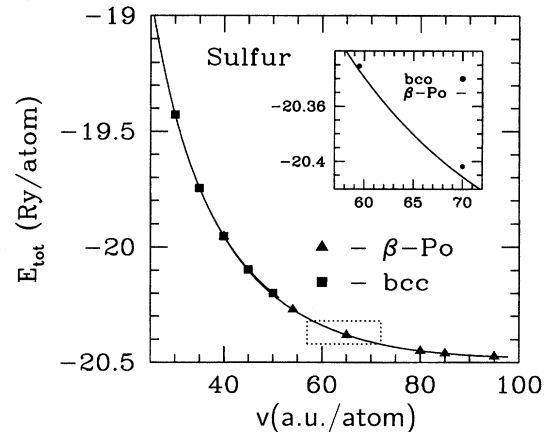


FIG. 1. Total-energy vs volume curves for β -Po and bcc phases of S obtained by a fit of the calculated energies to the Murnaghan equation of state. The triangles correspond to the calculated energies for the β -Po structure, the squares for the bcc structure. The inset shows a blowup of the region where the bco phase was found experimentally. The points in the inset are the total energies for the bco structure calculated by the minimization procedure.

Since our calculations converge within 1 mRy/atom and the minimization errors also do not exceed 1 mRy/atom, at this point we conclude that the LDA total energy of the considered model for the bco structure is higher than the LDA total energy of the β -Po phase at all volumes considered. Using the calculated values for the bulk modulus and the Debye model for the phonon dispersion, we estimated the zero-point motion energy to be about 1 mRy/atom for both structures; hence this contribution cannot change the obtained order of the phases. Thus our calculations do not reproduce the experimentally observed bco-to- β -Po structural phase transition for sulfur.

We note here that the deformation of the considered bco structure with the unequal zigzag bond lengths may have lower total energy than the structure for which our calculations were performed. But very thorough theoretical study of high-pressure phases of Te,¹⁰ in which the authors varied the zigzag bond lengths and performed both pseudopotential and all-electron LDA calculations resulted in similar conclusions. The LDA total energy of the bco phase of Te was found to be about 2 mRy/atom higher than the total energy of the β -Po phase. The authors attributed these results to the failure of the LDA to describe the weak bonds correctly.

For the parameter values $a=b=\sqrt{2}c$, $u=0.25$, the bco structure coincides with the bcc structure. Hence, we conclude that the bco structure has two minima, one, found by the minimization procedure and the other corresponding to the bcc structure. The total energies of these two phases are very close: at an atomic volume of $40 \text{ a.u.}^3/\text{atom}$ the difference of the total energies is only 5 mRy/atom. This difference increases to 9 mRy as we increase the pressure and decrease the atomic volume to $28 \text{ a.u.}^3/\text{atom}$. These results agree with the fact that the close-packed bcc structure becomes energetically more favorable at high pressure. The small energy difference between the two phases at the con-

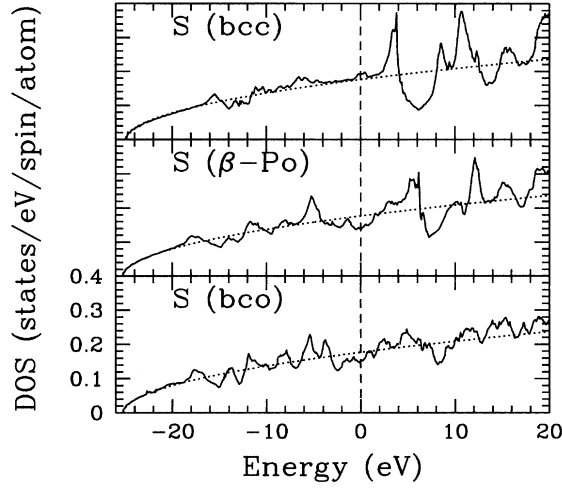


FIG. 2. The calculated LDA densities of states for the bcc, β -Po, and bco phases of sulfur at an atomic volume of 59.5 a.u.³/atom. The zero of energy corresponds to the Fermi energy. The broken line represents the density of states for a free electron gas with the same electron density and an effective mass of $1.11m_e$.

sidered pressure range is explained by the fact that the bco phase found by the minimization has lower band energy contribution to the total energy than the bcc phase.

The densities of states for the three structures considered are given in Fig. 2. These plots demonstrate the free-electron-like character of the valence electron wave functions for all three structures. The band masses m_b obtained from the density of states graphs are approximately $1.11m_e$ for all the structures considered. The position of the Fermi energy at the local minimum of the density of state curve makes the β -Po and bco structures favorable from the point of view of the band-energy contribution to the total energy. This conclusion agrees with the results of similar calculations for Te.⁹ At higher pressure the close-packed bcc structure becomes stable because of its lower Ewald energy.

The important difference between the electronic structures of the high-pressure phases of S and of the corresponding phases of Te is that at pressures and atomic separations characteristic of high-pressure phases of S there is no clear distinction between the bands formed by the s electrons and p electrons, whereas in the case of Te, these bands are well separated.⁹

III. ELECTRON-PHONON INTERACTION IN THE bcc PHASE OF SULFUR

A. Method

The calculations of the phonon dispersion and of the electron-phonon coupling constant λ are based on a fully self-consistent method,²¹ which does not require the rigid-ion approximation.²² This method uses the “frozen phonon” approach. The calculations are performed for a distorted supercell commensurate with the phonon wave vector \mathbf{q} for the phonon mode ν . For each phonon mode considered, we cal-

culate the frequency $\omega_{\mathbf{q}\nu}$ using the difference of the total energies for the distorted and undistorted crystals:

$$\omega_{\mathbf{q}\nu}^2 = \frac{2(E^{\text{dis}} - E^{\text{undis}})}{M u_{\mathbf{q}\nu}^2}, \quad (1)$$

where E^{dis} (E^{undis}) is the total energy per atom for the distorted (undistorted) crystal, M is the atomic mass, and $u_{\mathbf{q}\nu}^2$ is the average of the sum of the squares of the frozen phonon displacements.

The electron-phonon coupling constant $\lambda_{\mathbf{q}\nu}$ for coupling to each phonon mode (\mathbf{q}, ν) is defined as

$$\lambda_{\mathbf{q}\nu} = 2N(E_F) \frac{\langle\langle |g(n\mathbf{k}, n'\mathbf{k}'; \mathbf{q}\nu)|^2 \rangle\rangle}{\hbar \omega_{\mathbf{q}\nu}}. \quad (2)$$

Here $N(E_F)$ is the density of states per unit cell and per spin at the Fermi level E_F and $\langle\langle |g(n\mathbf{k}, n'\mathbf{k}'; \mathbf{q}\nu)|^2 \rangle\rangle$ denotes a double Fermi surface average of the square of the electron-phonon matrix element g ,²² given by the expression

$$g(n\mathbf{k}, n'\mathbf{k}'; \mathbf{q}\nu) = \left(\frac{\hbar \Omega_{\text{BZ}}}{2M \omega_{\mathbf{q}\nu}} \right)^{\frac{1}{2}} \left\langle \psi_{n\mathbf{k}}^0 \left| \epsilon_{\mathbf{q}\nu} \frac{\delta V}{\delta \mathbf{R}} \right| \psi_{n'\mathbf{k}'}^0 \right\rangle \times \delta(\mathbf{k} - \mathbf{k}' - \mathbf{q}), \quad (3)$$

where Ω_{BZ} is the volume of the Brillouin zone (BZ), $\epsilon_{\mathbf{q}\nu}$ is the phonon polarization vector, and $\delta V / \delta \mathbf{R}$ is the change in the self-consistent crystal potential caused by the phonon distortion. The double average is calculated using the Gaussian broadening method.²¹ More than 1000 special \mathbf{k} points in the irreducible part of the BZ have been used to compute this average. We also calculate the geometrical factor $\langle\langle \delta(\mathbf{k} - \mathbf{k}' - \mathbf{q}) \rangle\rangle$,²⁵ which depends on the geometry of the Fermi surface and characterizes the degree of nesting of the Fermi surface for a given phonon.

The electron-phonon coupling constant λ is expressed as a sum over different phonon modes ν of the BZ averages of $\lambda_{\mathbf{q}\nu}$.²⁶

$$\lambda = \frac{1}{\Omega_{\text{BZ}}} \sum_{\nu} \int d^3q \lambda_{\mathbf{q}\nu}. \quad (4)$$

We approximate this integral by taking a spherical average of the calculated $\lambda_{\mathbf{q}\nu}$ along the symmetry directions. The parameter λ can be used to estimate the superconducting transition temperature T_c by applying the McMillan^{27,28} equation:

$$T_c = \frac{\langle \omega \rangle}{1.2} \exp \left(\frac{-1.04(1 + \lambda)}{\lambda - \mu^* - 0.62\lambda \mu^*} \right). \quad (5)$$

Here $\langle \omega \rangle$ is an average phonon frequency defined by the expression

$$\langle \omega \rangle = \frac{\sum_{\mathbf{q}, \nu} \lambda_{\mathbf{q}\nu} \omega_{\mathbf{q}\nu}}{\sum_{\mathbf{q}, \nu} \lambda_{\mathbf{q}\nu}} \quad (6)$$

and μ^* is the screened Coulomb interaction coupling constant. Because of the nearly free-electron character of sulfur at high pressures, we estimate μ^* using the free-electron gas screening model.

TABLE I. The calculated phonon frequencies, electron-phonon coupling constants, and Fermi surface nesting factors for sulfur in the bcc structure. The letters L and T denote the longitudinal and transverse phonons. The polarization vector is along the $[1,-1,0]$ direction for the T_1 phonons and along the $[0,0,1]$ direction for the T_2 phonons.

Mode (\mathbf{q}, ν)	$\omega_{\mathbf{q}, \nu}$ (meV)	$\lambda_{\mathbf{q}, \nu}$	Geom. factor
$L_{\frac{1}{3}}[001]$	71.1	0.18	4.2
$T_{\frac{1}{3}}[001]$	29.6	0.68	
$L_{\frac{1}{2}}[001]$	93.5	0.15	3.2
$T_{\frac{1}{2}}[001]$	54.6	0.23	
$L_{\frac{2}{3}}[001]$	98.1	0.08	2.3
$T_{\frac{2}{3}}[001]$	72.4	0.15	
$[001]$	93.4	0.06	1.2
$L_{\frac{1}{6}}[110]$	58.6	0.25	4.6
$T_{1\frac{1}{6}}[110]$	25.0	0.36	
$T_{2\frac{1}{6}}[110]$	21.1	0.68	
$L_{\frac{1}{4}}[110]$	91.5	0.17	3.0
$T_{1\frac{1}{4}}[110]$	35.5	0.17	
$T_{2\frac{1}{4}}[110]$	32.9	0.44	
$L_{\frac{1}{3}}[110]$	111.2	0.12	2.3
$T_{1\frac{1}{3}}[110]$	32.2	0.24	
$T_{2\frac{1}{3}}[110]$	31.6	0.63	
$L_{\frac{1}{2}}[110]$	131.6	0.11	1.2
$T_{1\frac{1}{2}}[110]$	39.5	0.11	
$T_{2\frac{1}{2}}[110]$	43.4	0.40	
$L_{\frac{1}{4}}[111]$	98.7	0.12	7.4
$T_{\frac{1}{4}}[111]$	46.1	0.27	
$L_{\frac{1}{3}}[111]$	107.9	0.09	4.4
$T_{\frac{1}{3}}[111]$	57.9	0.21	
$\frac{1}{2}[111]$	86.9	0.15	3.6
$L_{\frac{2}{3}}[111]$	40.8	0.28	2.4
$T_{\frac{2}{3}}[111]$	99.4	0.14	

Approximating the transport electron-phonon coupling constant λ_{tr} by λ ,^{22,29} we also estimate the resistivity of metallic sulfur for temperatures of the order of the Debye temperature Θ_D using the high-temperature limit of Ziman's resistivity formula.²²

$$\rho = \frac{4\pi m_b k_B T}{ne^2 \hbar} \lambda_{tr}, \quad (7)$$

where m_b is a band mass and n is the number of electrons per unit volume.

B. Results and discussion

Using the frozen phonon method, we calculate the phonon frequencies and the electron-phonon coupling constants for the twelve \mathbf{q} points in the BZ of the high-pressure bcc phase of S. The calculations were performed for a lattice constant of 2.242 Å. According to our calculations, this lattice constant corresponds to a pressure of 584 GPa. Under such pressure the bcc phase of sulfur becomes stable. We expect that

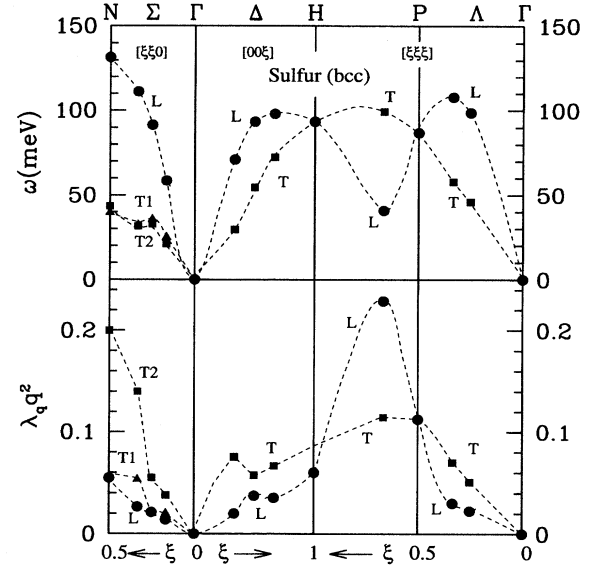


FIG. 3. The calculated phonon dispersion and the electron-phonon coupling constants $\lambda_{\mathbf{q}, \nu}$ for the high-pressure bcc phase of sulfur for an atomic volume of 5.631 Å³ and a calculated pressure of 584 GPa. The circles correspond to the longitudinal modes; squares and triangle correspond to the transverse modes. The lines are used as a guide for the eye only. The coupling constants $\lambda_{\mathbf{q}, \nu}$ are weighted with a phase space factor q^2 .

in the vicinity of the bcc-to- β -Po transition point there will be a stronger electron-phonon interaction and thus a larger coupling constant λ .

The results of our calculations are presented in Table I. The first column of this table specifies the phonon mode. The two transverse phonon modes for the wave vectors \mathbf{q} corresponding to the Δ and Λ directions are degenerate because of the symmetry of the crystal. All three phonon modes are degenerate at the H and P symmetry points. The calculated phonon frequencies $\omega_{\mathbf{q}, \nu}$ and the electron-phonon coupling constants $\lambda_{\mathbf{q}, \nu}$ are given in the second and third columns. The geometrical factor from the fourth column is defined in the preceding section. It describes the degree of Fermi surface nesting for a given phonon wave vector \mathbf{q} and does not depend on the polarization of the phonon.

The phonon dispersion curves and the electron-phonon coupling constants (weighted with a phase space factor q^2) for different phonon modes along the symmetry directions are given in Fig. 3. The phonon dispersion has several interesting features, namely, a sharp decrease of the frequency for the $L_{\frac{2}{3}}(1,1,1)$ phonon mode, close frequencies for two transverse phonons with wave vectors along the $[110]$ directions and a noticeable dip for the transverse phonons with $\frac{1}{3}(1,1,0)$ \mathbf{q} vector.

The dip in the frequency for the $L_{\frac{2}{3}}(1,1,1)$ phonon mode was observed experimentally for several bcc phases of group-IV metals²³ and was attributed to the general weakness of the bcc structure with respect to the so-called ω distortion.²⁴ We will argue that it is not related to the structural instability of the bcc phase near the bcc-to- β -Po phase transition.

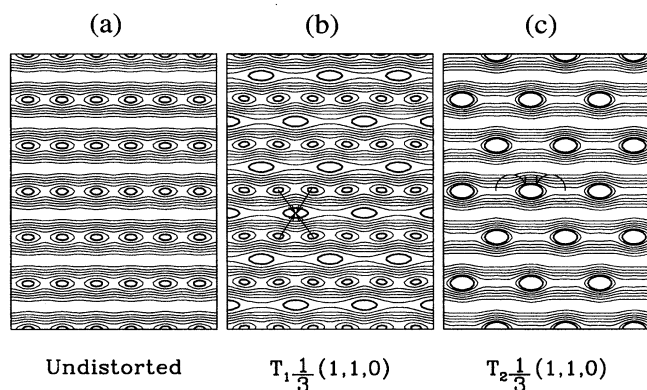


FIG. 4. The valence charge density for the undistorted (a), $T_1 \frac{1}{3}(1,1,0)$ -distorted (b), and $T_2 \frac{1}{3}(1,1,0)$ -distorted (c) bcc structure for the (101) plane between two planes of atoms. The amplitude of the distortions is 0.2 a.u. The maxima in the charge density correspond to the cross sections of the bonds. Both of the considered distortions lead to the change of the coordination number from eight to six by the disappearance of some of the bonds in case (c) and by the formation of new bonds in the previously empty space in case (b). The distortion (c) results in much larger charge transfer than the distortion (b).

The small difference between phonon frequencies for two transverse branches along $[110]$ direction is especially interesting, since the “bare” Ewald frequencies for these two modes are quite different. For example, at the N point the Ewald frequency of the T_2 mode with $[001]$ polarization is 2.6 times higher than the Ewald frequency of the T_1 mode with $[1\bar{1}0]$ polarization. Indeed, the experimental frequency measurements for group-IV metals approximately reproduce this ratio for the two transverse modes.²³ The fact that the calculated frequencies “dressed” with electron-phonon interaction are so close for sulfur indicates the existence of the strong electron-phonon interaction for the T_2 branch, in agreement with our electron-phonon coupling calculations.

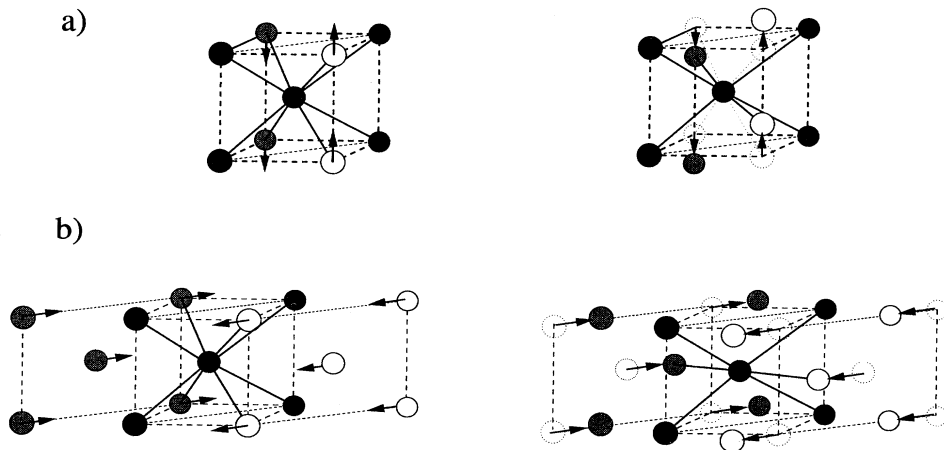


FIG. 5. A schematic picture of the $T_2 \frac{1}{3}(1,1,0)$ (a) and $T_1 \frac{1}{3}(1,1,0)$ (b) phonon distortions. The bonds are shown as solid lines. Both distortions lead to a change of the coordination number of the structure from eight to six. The distortion (a) results in the disappearance of one of the bonds, whereas in case (b) two bonds disappear and one new bond forms. The displacement of atoms in (b) are perpendicular to the bonds and it does not result in a significant charge transfer for small distortions (see Fig. 4). In (a) the charge transfer from the stretched into the compressed bond leads to the complete disappearance of the stretched bond even for relatively small distortions (Fig. 4).

To investigate the connection of $\frac{1}{3}(1,1,0)$ transverse phonon modes to the phase transition we considered the valence charge redistribution due to the lattice distortions corresponding to these phonons with relatively large amplitude, which we have chosen to be 0.2 a.u. (approximately 7% of the bond length). Figure 4 shows that both of these distortions produce a charge redistribution consistent with the change of the coordination number from eight to six during the bcc-to- β -Po phase transition. The charge transfer for the T_2 mode for which we observe complete disappearance of one of the bonds is much larger than for the T_1 mode. Using the notion of bonds we can explain this difference between two polarizations in the following way. The distortions corresponding to the T_1 phonons are perpendicular to the bonds of the bcc structure and thus result in bond bending with some charge transfer to the empty space between the bonds, whereas the T_2 phononlike distortions result in compression of some bonds and stretching of others with significant charge transfer from the stretched bonds to the compressed ones.

This change of the coordination number is further illustrated in Fig. 5. Cases (a) and (b) correspond to the $T_2 \frac{1}{3}(1,1,0)$ and $T_1 \frac{1}{3}(1,1,0)$ distortions. We see that the distorted structures are not exactly the β -Po phase, and we need some additional relaxation of the bond lengths and the bond angles to obtain the β -Po structure. The distortion (a) makes two of the three bond angles smaller. We recall here that during the bcc-to- β -Po phase transition all three bond angles become smaller.

The calculated pressure dependence of the frequency and the electron-phonon coupling constant for $T_2 \frac{1}{3}(1,1,0)$ and $L \frac{2}{3}(1,1,1)$ is given in Fig. 6. The increase in the electron-phonon interaction for the $L \frac{2}{3}(1,1,1)$ with pressure leads us to the conclusion that the strong electron-phonon interaction for this phonon mode is not related to the bcc-to- β -Po structural phase transition. The fast decrease of the electron-phonon interaction at higher pressure, where the bcc phase becomes stable, confirms our conclusion about the enhancement of the electron-phonon interaction for the $T_2 \frac{1}{3}(1,1,0)$ mode near the phase-transition point.

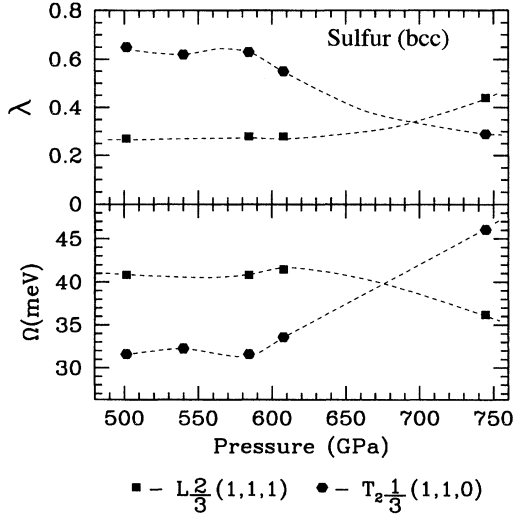


FIG. 6. The pressure dependence of the phonon frequency $\omega_{q\nu}$ and the electron-phonon coupling constant $\lambda_{q\nu}$ for $L_{\frac{2}{3}}^2(1,1,1)$ (square) and $T_{\frac{2}{3}}^1(1,1,0)$ (hexagon) phonon modes. The lines are used as a guide for the eye.

Using the results of our calculations, we now estimate the electron-phonon coupling constant λ . Knowing λ , we are able to estimate T_c using the McMillan equation (5) and the resistivity using the high-temperature limit of Ziman's resistivity formula. The average frequency $\langle\omega\rangle$ entering the McMillan equation calculated using the data from Table I is equal to 51.1 meV and corresponds to a temperature of 593 K. The electron-phonon coupling constant λ is evaluated by calculating the spherical averages of $\Sigma_{\nu}\lambda_{q\nu}$ along the considered high-symmetry directions and then finding their average with the weights equal to the number of the corresponding directions in the BZ. According to our calculations, λ is equal to 0.58.

To calculate T_c using the McMillan equation (5) the value of the Coulomb repulsion parameter μ^* is needed. Using the static Thomas-Fermi expression as an approximation for the dielectric function in S, we estimate μ^* to be 0.08. The value of T_c obtained from the McMillan equation using the parameters $\lambda=0.58$, $\mu^*=0.08$, and $\langle\omega\rangle=593$ K is 15 K.

This relatively high value of T_c is related to the enhancement of electron-phonon interaction near the structural phase transition, since, as we argued above, the important contribution to the electron-phonon coupling constant λ coming from the $T_{\frac{2}{3}}^1(1,1,0)$ phonon modes is related to the vicinity of

the bcc-to- β -Po structural phase transition. The experimental study of the pressure dependence of T_c for Te (Ref. 14) showed that T_c abruptly increases from 2.5 to 7.4 K during the β -Po-to-bcc phase transition and then rapidly decreases to 4.5 K.

Even near the phase-transition point the bcc phase of sulfur is a very good conductor. Using the calculated value of λ as an approximation for λ_{tr} , we calculate high-temperature behavior of the electrical resistivity. For the bcc phase at a pressure of 585 GPa the high-temperature limit of Ziman's resistivity formula gives $\rho(T)=3.5\times 10^{-9}(\Omega\text{ cm/K})T$. For $T=600$ K, we obtain $\rho=2.1\times 10^{-6}\Omega\text{ cm}$, which is comparable with the resistivity of silver at room temperature ($\rho=1.6\times 10^{-6}\Omega\text{ cm}$). We expect even lower resistivity for pressures that are not so close to the transition pressure. For Te, the resistivity at the β -Po-to-bcc transition point increases by about 15%.¹⁴

IV. CONCLUSION

Pseudopotential total-energy calculations are performed for three-high pressure phases of sulfur. The phase transition from the β -Po to the bcc phase at a pressure of 545 GPa is predicted; however, we are not able to reproduce the experimentally observed bcc-to- β -Po structural phase transition, since, according to our calculations, the bcc phase is higher in energy than by the β -Po phase.

The frozen phonon calculations of the phonon dispersion and the phonon-electron coupling for the bcc phase of sulfur indicate that at high pressure sulfur is a very good metal with low resistivity. We estimate the value of the superconducting T_c for the bcc phase of sulfur near the β -Po-to-bcc structural transition to be 15 K. The effects of the vicinity of the structural bcc-to- β -Po phase transition on the enhancement of the electron-phonon interaction are examined.

ACKNOWLEDGMENTS

We would like to thank Professor A. Ruoff for providing experimental data prior to publication and Dr. V. Crespi for very useful discussions. This work was supported by National Science Foundation Grant No. DMR91-20269 and by the Director, Office of Energy Research, Office of Basic Energy Sciences, Materials Sciences Division of the U.S. Department of Energy under Contract No. DE-AC03-76SF00098. Cray Computer time was provided by the National Science Foundation at the National Center for Supercomputing Applications, and the National Science Foundation at the Pittsburgh Supercomputing Center.

¹G. Parthasarathy and W. B. Holzapfel, Phys. Rev. B **37**, 8499 (1988).

²G. Parthasarathy and W. B. Holzapfel, Phys. Rev. B **38**, 10 105 (1988).

³H. Luo, S. Desgreniers, Y. K. Vohra, and A. L. Ruoff, Phys. Rev. Lett. **67**, 2998 (1991).

⁴Y. Akahama, M. Kobayashi, and H. Kawamura, Phys. Rev. B **47**, 20 (1993).

⁵H. Luo and A. L. Ruoff, Phys. Rev. B **48**, 569 (1993).

⁶Y. Akahama, M. Kobayashi, and H. Kawamura, Phys. Rev. B **48**, 6862 (1993).

⁷H. Luo, R. G. Greene, and A. L. Ruoff, Phys. Rev. Lett. **71**, 2943 (1993).

⁸G. Doerre and J. D. Joannopoulos, Phys. Rev. Lett. **43**, 1040 (1979).

- ⁹A. Nishikawa, K. Niizeki, and K. Shindo, *Jpn. J. Appl. Phys.* **32-1**, 48 (1993).
- ¹⁰F. Kirchoff, N. Bingelli, and G. Galli, *Phys. Rev. B* **50**, 9063 (1994).
- ¹¹J. Ihm, A. Zunger, and M. L. Cohen, *J. Phys. C* **12**, 4409 (1979).
- ¹²I. V. Berman, Zh. I. Binzarov, and P. Kurkin, *Sov. Phys. Solid State* **14**, 2192 (1973).
- ¹³F. P. Bundy and K. J. Dunn, *Phys. Rev. B* **22**, 3157 (1980).
- ¹⁴Y. Akahama, M. Kobayashi, and H. Kawamura, *Solid State Commun.* **84**, 803 (1992).
- ¹⁵José L. Martins, N. Troullier, and S.-H. Wei, *Phys. Rev. B* **43**, 2213 (1991).
- ¹⁶D. M. Ceperley and B. J. Alder, *Phys. Rev. Lett.* **45**, 566 (1980).
- ¹⁷D. J. Chadi and M. L. Cohen, *Phys. Rev. B* **8**, 5747 (1973).
- ¹⁸H. J. Monkhorst and J. D. Pack, *Phys. Rev. B* **13**, 5188 (1976).
- ¹⁹F. D. Murnaghan, *Proc. Natl. Acad. Sci. U.S.A.* **30**, 244 (1944).
- ²⁰A. L. Ruoff (private communication).
- ²¹P. K. Lam, M. M. Dacorogna, and M. L. Cohen, *Phys. Rev. B* **34**, 4996 (1986).
- ²²G. Grimvall, *The Electron-Phonon Interaction in Metals* (North-Holland, Amsterdam, 1981).
- ²³W. Petry *et al.*, *Phys. Rev. B* **43**, 10 933 (1991).
- ²⁴D. De Fontaine and O. Buck, *Philos. Mag.* **27**, 967 (1973).
- ²⁵J. L. Martins and M. L. Cohen, *Phys. Rev. B* **37**, 3304 (1988).
- ²⁶K. J. Chang and M. L. Cohen, *Phys. Rev. B* **34**, 4552 (1986).
- ²⁷W. L. McMillan, *Phys. Rev.* **167**, 331 (1968).
- ²⁸P. B. Allen and R. C. Dynes, *Phys. Rev. B* **12**, 905 (1975).
- ²⁹V. H. Crespi and M. L. Cohen, *Solid State Commun.* **81**, 187 (1992).